

# Characteristics of NO<sub>x</sub> emission from Chinese coal-fired power plants equipped with new technologies



Zizhen Ma<sup>a</sup>, Jianguo Deng<sup>a</sup>, Zhen Li<sup>a</sup>, Qing Li<sup>a</sup>, Ping Zhao<sup>b</sup>, Ligu Wang<sup>b</sup>, Yezhu Sun<sup>b</sup>, Hongxian Zheng<sup>b</sup>, Li Pan<sup>c</sup>, Shun Zhao<sup>c</sup>, Jingkun Jiang<sup>a, \*\*</sup>, Shuxiao Wang<sup>a, d</sup>, Lei Duan<sup>a, d, \*</sup>

<sup>a</sup> State Key Laboratory of Environmental Simulation and Pollution Control, School of Environment, Tsinghua University, Beijing 100084, China

<sup>b</sup> Huaneng Power International Inc., Beijing 100031, China

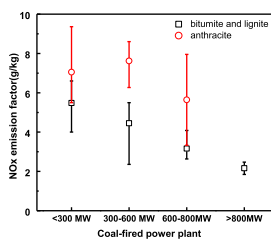
<sup>c</sup> Huaneng Yuhuan Power Plant, Yuhuan 317604, China

<sup>d</sup> Collaborative Innovation Centre for Regional Environmental Quality, Tsinghua University, Beijing 10084, China

## HIGHLIGHTS

- NO<sub>x</sub> emission factors of coal-fired power plant were updated by field measurement.
- Newer units with higher installed capacity have much lower NO<sub>x</sub> emission factors.
- NO<sub>2</sub>/NO<sub>x</sub> ratio remains under 5% after installing air pollution control devices such as SCR.

## GRAPHICAL ABSTRACT



## ARTICLE INFO

### Article history:

Received 24 November 2015

Received in revised form

3 February 2016

Accepted 3 February 2016

Available online 4 February 2016

### Keywords:

Coal-fired power plants

NO<sub>2</sub>/NO<sub>x</sub> ratio

NO<sub>x</sub> emission factor

Selective catalytic reduction (SCR)

## ABSTRACT

Coal combustion in coal-fired power plants is one of the important anthropogenic NO<sub>x</sub> sources, especially in China. Many policies and methods aiming at reducing pollutants, such as increasing installed capacity and installing air pollution control devices (APCDs), especially selective catalytic reduction (SCR) units, could alter NO<sub>x</sub> emission characteristics (NO<sub>x</sub> concentration, NO<sub>2</sub>/NO<sub>x</sub> ratio, and NO<sub>x</sub> emission factor). This study reported the NO<sub>x</sub> characteristics of eight new coal-fired power-generating units with different boiler patterns, installed capacities, operating loads, and coal types. The results showed that larger units produced less NO<sub>x</sub>, and anthracite combustion generated more NO<sub>x</sub> than bitumite and lignite combustion. During formation, the NO<sub>x</sub> emission factors varied from 1.81 to 6.14 g/kg, much lower than those of older units at similar scales. This implies that NO<sub>x</sub> emissions of current and future units could be overestimated if they are based on outdated emission factors. In addition, APCDs, especially SCR, greatly decreased NO<sub>x</sub> emissions, but increased NO<sub>2</sub>/NO<sub>x</sub> ratios. Regardless, the NO<sub>2</sub>/NO<sub>x</sub> ratios were lower than 5%, in accordance with the guidelines and supporting the current method for calculating NO<sub>x</sub> emissions from coal-fired power plants that ignore NO<sub>2</sub>.

© 2016 Elsevier Ltd. All rights reserved.

\* Corresponding author. State Key Laboratory of Environmental Simulation and Pollution Control, School of Environment, Tsinghua University, Beijing 100084, China.

\*\* Corresponding author.

E-mail addresses: [jiangjk@tsinghua.edu.cn](mailto:jiangjk@tsinghua.edu.cn) (J. Jiang), [lduan@tsinghua.edu.cn](mailto:lduan@tsinghua.edu.cn) (L. Duan).

## 1. Introduction

Coal-fired power generation is the main source of electricity in China. In 2014, China accounted for 50.6% of the total world coal consumption, while more than 50% of Chinese coal was used to

generate power, much higher than the world average (British Petroleum, 2015). However, coal combustion increases the atmospheric environmental burden by emitting contaminants, such as sulphur dioxide, nitrogen oxides (NO<sub>x</sub>), and particulate matter. Therefore, policies on energy conservation and emissions abatement have been implemented in China to control industrial air pollution, especially from coal-fired power plants. Most units with installed capacities less than 50 MW were closed before 2003, and units with installed capacities less than 200 MW began to close in 2007 (China State Council, 1999, 2007). The required minimum capacity of newly constructed units is 300 MW. As a result, units with 300-MW and 600-MW capacities increase very fast and predominate in China, accounting for 33.8 and 49.3% of the total capacity in 2010, respectively. In the same year, 1000-MW units increased to 6% (China State Electricity Regulatory Commission, 2011). Most new units have been installed with low NO<sub>x</sub> burners (LNBS). These improvements could change the characteristics of NO<sub>x</sub> emissions. In addition, air pollution control devices (APCDs) have been installed in most coal-fired power plants in the past decade. Since the end of 2012, electrostatic precipitators (ESP) and flue gas desulfurization (FGD) units have been installed in most coal-fired power plants, and selective catalytic reduction (SCR) units were installed in 80% of coal-fired power plants by 2014 (Xu et al., 2009; Wang et al., 2010; Wang and Hao, 2012; Zhao et al., 2013; Wang et al., 2014). These devices could alter NO<sub>x</sub> emission characteristics. For instance, there is a side reaction that NO<sub>2</sub> is generated on the surface of catalysts by oxidization of NO, even though most NO is reduced to N<sub>2</sub> (Adamowska-Teyssier et al., 2015). Furthermore, the composition of NO<sub>x</sub> can be affected by ESP and FGD, because NO can be oxidized in these two devices, but NO<sub>2</sub> can be absorbed by FGD slurry (Sun et al., 2013).

Nitric oxide is widely reported to be the dominant form of NO<sub>x</sub> from coal combustion, while the percentage of NO<sub>2</sub> in NO<sub>x</sub> is less than 5% (Flagan and Seinfeld, 1988; William, 1988). NO<sub>x</sub> emissions from coal-fired power plants are usually calculated by multiplying the measured NO by a fixed coefficient of 1.53, the molecular weight ratio of NO<sub>2</sub>/NO, without considering the minor contribution of NO<sub>2</sub> to NO<sub>x</sub>. This method, as well as NO<sub>x</sub> emission factors, should be re-evaluated, because new coal-fired power plants in China might have different quantities and compositions of NO<sub>x</sub> emissions. This study characterised NO<sub>x</sub> generated and emitted from new power plants with different boiler types, installed capacities, operating loads, and coal types, as well as APCD installations, especially SCR units. Such information could support policy-making on cleaner power generation from coal-fired power plants, which are irreplaceable in many countries, including China, India, USA, Canada, and Japan.

## 2. Methodology

### 2.1. Power plant descriptions

Eight coal-fired power-generating units (Table 1) were chosen to investigate NO<sub>x</sub> emission characteristics. All units were installed with LNBS and SCR units to reduce NO<sub>x</sub> emissions, with the exception of YL3 without a LNB. Coal type, installed capacity, and operating load of the units were considered to be factors controlling NO<sub>x</sub> generation. Coal types included bitumite, anthracite, and lignite (Table 1). Boiler capacity was divided into three grades, >800, 600–800, and <600 MW. Three load conditions, 100, 75, and 50%, were controlled in the investigation.

### 2.2. Sampling method and analysis

For each coal-fired unit, flue gas NO and NO<sub>2</sub> concentrations were analysed at the SCR inlet, SCR outlet, and FGD outlet to determine the characteristics of NO<sub>x</sub> formation (SCR inlet) and emissions (FGD outlet) and to identify the impacts of SCR and FGD on NO<sub>x</sub> characteristics (Fig. 1a). The sampling system was designed according to Method 7E of the United States Environmental Protection Agency (USEPA, 2014) (Fig. 1b). The flue gas was pumped from the chimney through a venturi dilutor, where N<sub>2</sub> was mixed with the gas, and the flue gas particles were removed by a filter. Then, the cooled and diluted gas was aspirated into a NO<sub>x</sub> analyser (Model 42i, Thermo Scientific), using chemiluminescence to measure NO and NO<sub>2</sub> concentrations. A flue gas analyser (Testo 350, Testo, USA) was used to measure NO concentrations synchronously for data inter-comparisons.

For quality assurance and quality control, the NO<sub>x</sub> analyser was calibrated with zero gas and standard NO<sub>x</sub> gas (mixed with certain percentages of NO and NO<sub>2</sub>) under laboratory conditions and calibrated with standard NO<sub>x</sub> gas on-site before measurement. The dilutor and flue gas analyser were also calibrated in the laboratory.

The NO<sub>x</sub> emission factor was calculated using Equation (1):

$$EF = \frac{\rho \times Q \times 10^{-3}}{B} \quad (1)$$

where EF is the emission factor of NO<sub>x</sub> (g/kg);  $\rho$  is the measured concentration of NO<sub>x</sub> in flue gas (mg/Nm<sup>3</sup>);  $Q$  is the flow rate of dry flue gas in standard conditions (Nm<sup>3</sup>/h); and  $B$  is the feeding rate of coal (kg/h). Real-time data from tested coal-fired power plants were used to determine  $Q$  and  $B$ .

## 3. Results and discussion

### 3.1. NO<sub>x</sub> concentrations and NO<sub>2</sub>/NO<sub>x</sub> ratios

All measurement results are shown in Table 2. The NO concentrations measured using the Thermo Scientific 42i and Testo 350 at

**Table 1**  
Parameters of tested units and coal used.

Number	Burner type	Capacity (MW)	APCDs	Coal	Total moisture (%)	Ash (%)	Volatile matter (%)	Total sulphur (%)	Heat value (MJ/kg)
YH1	Tangential	1000	LNB + SCR + ESP + FGD	Bitumite	–	9.50	42.9	0.56	21.4
YH3	Tangential	1000	LNB + SCR + ESP + FGD	Bitumite	–	10.2	41.8	0.63	21.7
CX2	Tangential	660	LNB + SCR + ESP + FGD	Bitumite	16.8	12.0	26.5	0.50	21.3
SA2	W-Flame	350	LNB + SCR + ESP + FGD	Anthracite	10.5	26.5	14.8	1.94	21.9
SA3	W-Flame	330	LNB + SCR + ESP + FGD	Anthracite	11.2	23.4	13.8	1.49	22.7
YK2	Tangential	660	LNB + SCR + ESP + FGD	Lignite	24.5	7.84	43.7	0.19	19.9
YL3	Tangential	300	SCR + ESP + FGD	Bitumite	7.08	29.7	22.7	1.48	21.5
YL5	Wall	300	LNB + SCR + EBP* + FGD	Bitumite	10.0	26.0	37.9	0.89	20.7

\*EBP: Electrostatic-bag precipitator.

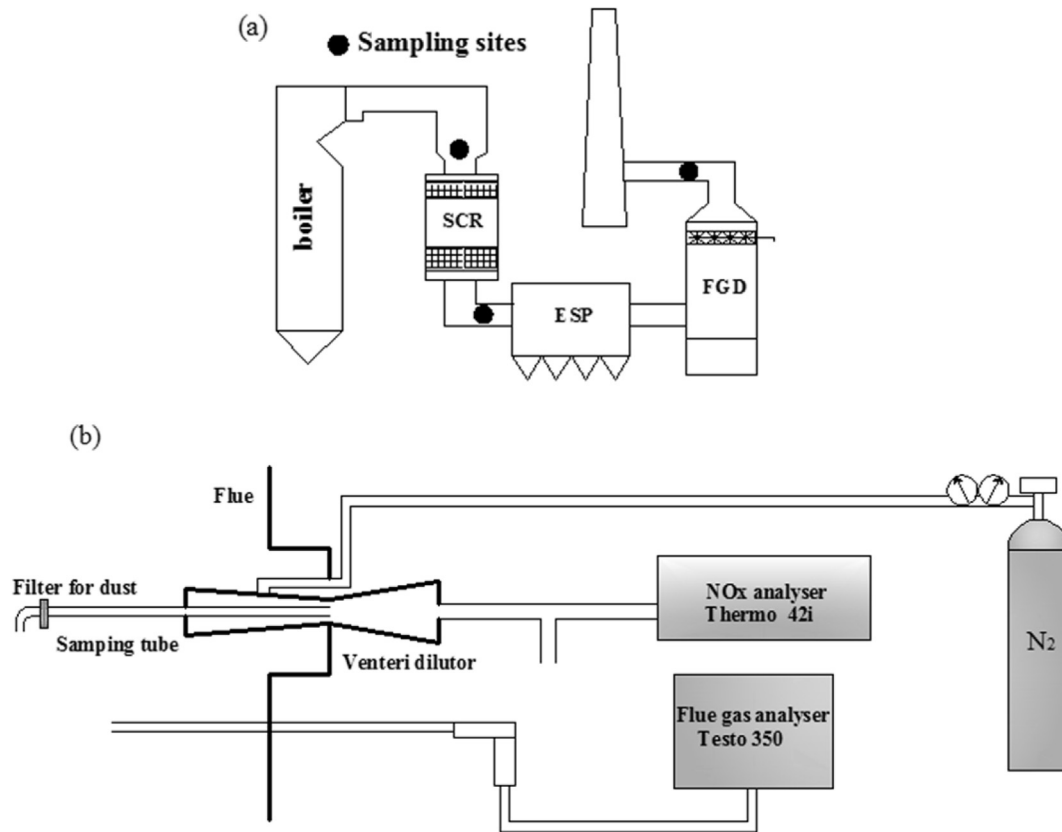


Fig. 1. Sampling sites (a) and schematic of sampling methods (b).

**Table 2**  
NO<sub>x</sub> concentrations (ppm) and NO<sub>2</sub>/NO<sub>x</sub> ratios (%) at different power plants.

Units	Item	Load								
		100%			75%			50%		
		SCR in	SCR out	FGD out	SCR in	SCR out	FGD out	SCR in	SCR out	FGD out
YH1	NO	146	28.7	24.2	85.0	16.8	18.4	107	–	18.7
	NO <sub>2</sub>	1.40	0.50	0.78	1.28	0.64	0.45	1.83	–	0.45
	NO <sub>2</sub> /NO <sub>x</sub>	0.95	1.70	3.10	1.48	3.68	2.40	1.68	–	2.30
YH3	NO	117	22.2	11.7	–	–	10.9	–	–	10.6
	NO <sub>2</sub>	0.85	0.69	0.57	–	–	0.28	–	–	0.21
	NO <sub>2</sub> /NO <sub>x</sub>	0.72	3.01	4.70	–	–	2.50	–	–	1.90
CX2	NO	100	11.1	15.0	–	–	5.00	–	–	–
	NO <sub>2</sub>	1.63	0.19	0.30	–	–	0.40	–	–	–
	NO <sub>2</sub> /NO <sub>x</sub>	1.60	1.64	2.00	–	–	7.40	–	–	–
SA2	NO	350	24.0	33.2	318	13.1	24.4	–	–	–
	NO <sub>2</sub>	3.93	0.34	1.22	3.23	0.35	0.90	–	–	–
	NO <sub>2</sub> /NO <sub>x</sub>	1.11	1.40	3.50	1.01	2.60	3.50	–	–	–
SA3	NO	437	138	40.9	429	102	34.5	–	–	–
	NO <sub>2</sub>	4.55	2.05	1.57	4.89	1.33	1.76	–	–	–
	NO <sub>2</sub> /NO <sub>x</sub>	1.03	1.47	3.70	1.10	1.30	4.80	–	–	–
YK2	NO	160	35.7	29.4	166	12.5	18.0	–	–	–
	NO <sub>2</sub>	2.07	0.49	1.87	0.95	0.24	1.00	–	–	–
	NO <sub>2</sub> /NO <sub>x</sub>	1.28	1.34	5.90	0.57	1.88	5.20	–	–	–
YL3	NO	479	97.0	84.2	397	59.8	39.8	367	39.2	29.1
	NO <sub>2</sub>	4.26	0.92	1.55	3.05	1.47	0.94	2.34	0.79	0.48
	NO <sub>2</sub> /NO <sub>x</sub>	0.88	0.94	1.80	0.76	2.39	2.30	0.63	1.98	1.60
YL5	NO	158	27.4	23.9	189	16.4	14.9	162	8.60	8.80
	NO <sub>2</sub>	1.60	0.58	0.56	2.46	0.20	0.38	1.36	0.17	0.16
	NO <sub>2</sub> /NO <sub>x</sub>	1.00	2.06	2.30	1.29	1.21	2.40	0.83	1.94	1.70

the same sampling site showed a strong correlation, with a slope of 1.007 and  $R^2$  of 0.9996.

Operated at 100% load capacity, the average NO concentration at

the SCR inlet was 243 ppm (range 100–479 ppm), while the average NO<sub>2</sub> concentration was 2.53 ppm (range 0.85–4.26 ppm). Compared with NO and NO<sub>2</sub>, other forms of NO<sub>x</sub> were low enough

to be neglected, so the ratios ( $\text{NO}_2/\text{NO}_x$ ) were calculated to vary from 0.72 to 1.60%. At the SCR outlet, the average NO and the average  $\text{NO}_2$  concentrations were 48.0 ppm (range 11.1–137 ppm) and 0.72 ppm (range 0.19–2.05 ppm), respectively. The corresponding average  $\text{NO}_2/\text{NO}_x$  ratios at the SCR outlet were 1.47% (range 0.94–3.01)%. At the FGD outlet, the average NO and the average  $\text{NO}_2$  concentrations were 32.8 ppm (range 11.7–84.2 ppm) and 1.05 ppm (range 0.30–1.87 ppm), respectively. Correspondingly, the average  $\text{NO}_2/\text{NO}_x$  ratio was 3.10% (range 1.22–5.90%).

The characteristics of  $\text{NO}_x$  differed slightly among operating loads. Operating at 75% load capacity, the average NO and  $\text{NO}_2$  concentrations at the SCR inlet were 264 and 2.64 ppm, respectively, and the average  $\text{NO}_2/\text{NO}_x$  ratio was 0.99%. At the SCR outlet, the average NO and  $\text{NO}_2$  concentrations were decreased to 36.8 and 0.70 ppm, respectively, while the average  $\text{NO}_2/\text{NO}_x$  ratio increased to 1.88%. At the FGD outlet, the average NO concentration declined, whereas the average  $\text{NO}_2$  concentration and  $\text{NO}_2/\text{NO}_x$  ratio increased.

Operating at 50% load capacity, the average NO and  $\text{NO}_2$  concentrations at the SCR inlet were 212 and 1.84 ppm, respectively, and the average  $\text{NO}_2/\text{NO}_x$  ratio was 0.86%. At the SCR and FGD outlets, the average  $\text{NO}_2$  concentrations were 23.6 and 16.8 ppm, respectively, while the average NO concentrations were 0.48 and 0.43 ppm, respectively. The  $\text{NO}_2/\text{NO}_x$  ratios were 1.97 and 1.90%, respectively.

In unit YL3, the only unit without a LNB, the NO and  $\text{NO}_2$  concentrations at the SCR inlet (479 and 4.26 ppm, respectively) were much higher than those of the other units, but the  $\text{NO}_2/\text{NO}_x$  ratio at the SCR inlet was around 1%, similar to the other units.

### 3.2. Emission factors of $\text{NO}_x$ at formation

Most of the units, especially those with capacities >300 MW, have been installed with LNBs to meet rigorous  $\text{NO}_x$  emission requirements. Under full load conditions,  $\text{NO}_x$  emission factors at the SCR inlet for units with a LNB in this study varied from 1.94 to 6.27 g/kg, much lower than that without a LNB (8.14 g/kg). Moreover, the  $\text{NO}_x$  emission factors of the new units in this study were much lower than those of previous units with LNBs of similar scales (Fig. 2) (Zhao et al., 2010; Lei, 2012; USEPA, 2014; Sun, 2015). The emission factors applied in most current emission inventory studies (Zhao et al., 2013) mainly come from Zhao et al. (2010),

which reported the emission factors according to installed capacity (<300 and  $\geq$ 300 MW), LNB installation or not, and burner type. For units with LNB burning bitumite and lignite, the emission factors used in the current inventory were 4.70 g/kg and 5.20 g/kg for tangential burner and wall-fired burner respectively (Zhao et al., 2010). In comparison, the  $\text{NO}_x$  emission factors were 2.29 g/kg (the average of 2.64 g/kg for 600–800 MW and 1.94 g/kg for >800 MW) for tangential burner and 2.36 g/kg (for units in the grade of 300–600 MW) for wall-fired burner, respectively, about 52% and 55% lower. In addition, the emission factor of the W-flame burners with LNB measured in this study (6.27 g/kg for units in grade of 300–600 MW) was about 44% lower than the value adopted in the current inventory (11.2 g/kg).

The main reason for the decrease in emission factors may be the improvement of LNB technology. Generally, the  $\text{NO}_x$  removal efficiency of LNB is in the range of 30–50% (Wang et al., 2011). The efficiency can be improved by as much as 40% by some new design of LNB, such as the optimized swirl burners (Zhou et al., 2014). For bitumite combustion in 100–300 MW units without LNB, the  $\text{NO}_x$  emission factors summarized by Zhao (2008) and Sun (2015) were in the range of 6.1–9.13 g/kg, which contains the value in this study (8.14 g/kg).

Considering the fast increasing occupancy of new units with lower  $\text{NO}_x$  emission factors, current and future  $\text{NO}_x$  emissions from coal-fired power plants in China could be overestimated if they are based on outdated  $\text{NO}_x$  emission factors. The  $\text{NO}_x$  emission factor used for the earliest emission inventory  $\text{NO}_x$  in China was 12.4 g/kg, which took no consideration of the variation in installed capacity or LNB installation (Tian et al., 2001). The  $\text{NO}_x$  emission factor used for later emission inventory decreased to 5.55–10.5 g/kg, depending on installed capacity (<100 MW, 100–300 MW, and 300–600 MW) and LNB (installed or not) (Zhang et al., 2007). More recently, the  $\text{NO}_x$  emission factor used was in the range of 4.00–11.2 g/kg, depending on not only installed capacity and LNB, but also coal type and burner type (Zhao et al., 2013). Obviously, the  $\text{NO}_x$  emission factor should further decrease when consider the very low emission level (2.03–2.81 g/kg) of new units with installed capacity higher than 800 MW (this study; Lei, 2012).

### 3.3. Factors of $\text{NO}_x$ formation

The seven coal-fired units equipped with a LNB and SCR unit

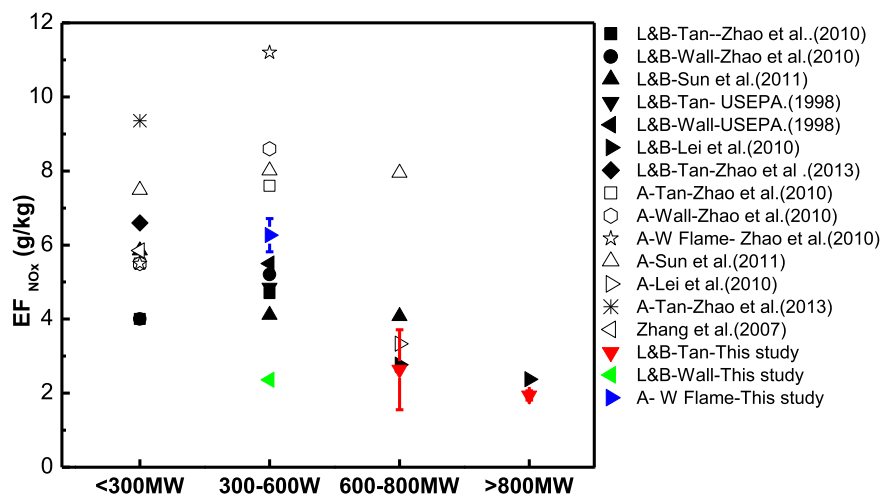


Fig. 2.  $\text{NO}_x$  emission factors of coal-fired power plants obtained from different studies. All results are from units installed with a LNB. L&B: Lignite or bitumite; A: anthracite; Tan: tangential burner; Wall: wall burner; W flame: W flame burner.

were classified into three grades according to the installed capacity, <600, 600–800, and >800 MW. At 100% load, the units with <600-MW installed capacities had the highest NO<sub>x</sub> concentrations (averagely 481 ppm) and NO<sub>x</sub> emission factors (averagely 4.97 g/kg). The NO<sub>x</sub> concentrations of 600–800 MW and >800 MW units were similar (199 ppm and 200 ppm in average, respectively), but the NO<sub>x</sub> emission factor of >800 MW units (averagely 1.94 g/kg) was lower than that of 600–800 MW units (averagely 2.63 g/kg) (Fig. 3a), indicating that larger units produced more NO<sub>x</sub> per unit of coal fired than smaller ones (Wang et al., 2009). Units with capacities of 600–800 MW had the highest NO<sub>2</sub>/NO<sub>x</sub> ratios at formation, while the >800 MW units had the lowest. All of the ratios calculated in this study were less than 2%, in accordance with results from the USEPA (USEPA, 1998). Therefore, the effect of installed capacity on NO<sub>2</sub>/NO<sub>x</sub> ratio is likely insignificant.

Operating load affects NO<sub>x</sub> concentration by altering the temperature and oxygen content of flue gas (Li et al., 2011). Since NO<sub>x</sub>

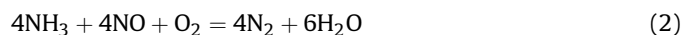
(mostly NO) generated during coal combustion comes mainly from either the reaction of N<sub>2</sub> with O<sub>2</sub> (called thermal-NO<sub>x</sub>) or the oxidation of fuel containing N (called fuel-NO<sub>x</sub>), flue gas temperature and O<sub>2</sub> concentration are key factors determining NO<sub>x</sub> formation (Flagan and Seinfeld, 1988; William, 1988). As load decreases, flue gas temperature decreases, resulting in less thermal-NO<sub>x</sub> and fuel-NO<sub>x</sub> formation. However, the air excess factor likely increases as load decreases, resulting in greater NO and NO<sub>2</sub> generation (Li et al., 2011). The integrated consequence of decreasing temperature and increasing oxygen content could cause unpredicted variations in NO<sub>x</sub> characteristics. This study showed that NO<sub>x</sub> concentrations decreased with decreasing operating load, but NO<sub>x</sub> emission factors increased slightly at 75% load and then decreased at 50% load (Fig. 3b). The minimum and maximum NO<sub>2</sub>/NO<sub>x</sub> ratios occurred at 75 and 100% loads, respectively; however, all NO<sub>2</sub>/NO<sub>x</sub> ratios were below 2%, which indicated that operating load conditions had little influence on the NO<sub>2</sub>/NO<sub>x</sub> ratios.

Fuel type is another factor that affects NO<sub>x</sub> formation. At 100% load, the NO<sub>x</sub> concentration and NO<sub>x</sub> emission factor from anthracite combustion were 397 ppm and 6.27 g/kg, respectively, higher than those from other coal types (Fig. 3c) and in agreement with other studies (Zhao et al., 2010; Lei, 2012; Sun, 2015). This can be attributed to the higher temperature of anthracite combustion than those of bitumite and lignite combustion (Fan et al., 2010; You et al., 2011). The NO<sub>2</sub>/NO<sub>x</sub> ratios of the three coal types were all less than 2%, implying that coal type had little effect on the NO<sub>2</sub>/NO<sub>x</sub> ratio.

#### 3.4. Effects of APCDs on NO<sub>x</sub> emissions

The NO<sub>x</sub> characteristics were affected by SCR, as 78–94% of NO<sub>x</sub> was reduced to N<sub>2</sub> (Fig. 4). The concentrations of NO<sub>2</sub> and NO in flue gas at all three operating loads at the SCR outlet decreased by 72–73 and 80–87%, respectively. By consequence, the NO<sub>x</sub> emission factors much declined between the SCR inlet and SCR outlet.

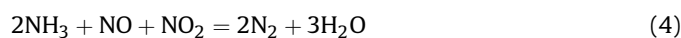
In this study, the NO<sub>2</sub>/NO<sub>x</sub> ratios were 43, 90, and 127% higher after SCR than before at 100, 75, and 50% loads, respectively (Fig. 4). Normally, NO<sub>2</sub> formation by oxidation of NO, which is easy at room temperature, is insignificant at flue gas temperature above 800K at which the production of NO invariably exceed NO<sub>2</sub> (Flagan and Seinfeld, 1988). However, the present of SCR may theoretically accelerate the oxidation. According to the mechanism of SCR, most NO is removed by the standard SCR reaction:



In addition, some NO is first converted to NO<sub>2</sub> by O<sub>2</sub>, accelerated by the SCR catalyst around 350 °C (Olsson et al., 1999):



The original and newly generated NO<sub>2</sub> can be removed according to the fast SCR reaction:



Therefore, the NO<sub>2</sub>/NO<sub>x</sub> ratio at the SCR outlet might differ from that at the SCR inlet because of consumption or generation of NO<sub>2</sub>. The increasing NO<sub>2</sub>/NO<sub>x</sub> ratios by SCR in this study implied that the newly generated NO<sub>2</sub> was not completely consumed by SCR (Busca et al., 1998; Koebel et al., 2001; Ciardelli et al., 2004; Adamowska-Teyssier et al., 2015). However, all NO<sub>2</sub>/NO<sub>x</sub> ratios were within 2% after SCR (Fig. 4), and the removal efficiency of NO<sub>x</sub> did not have a clear effect on the NO<sub>2</sub>/NO<sub>x</sub> ratio (Fig. 5).

The concentrations of NO<sub>2</sub> increased slightly, and NO concentrations decreased at the FGD outlet in comparison with those at

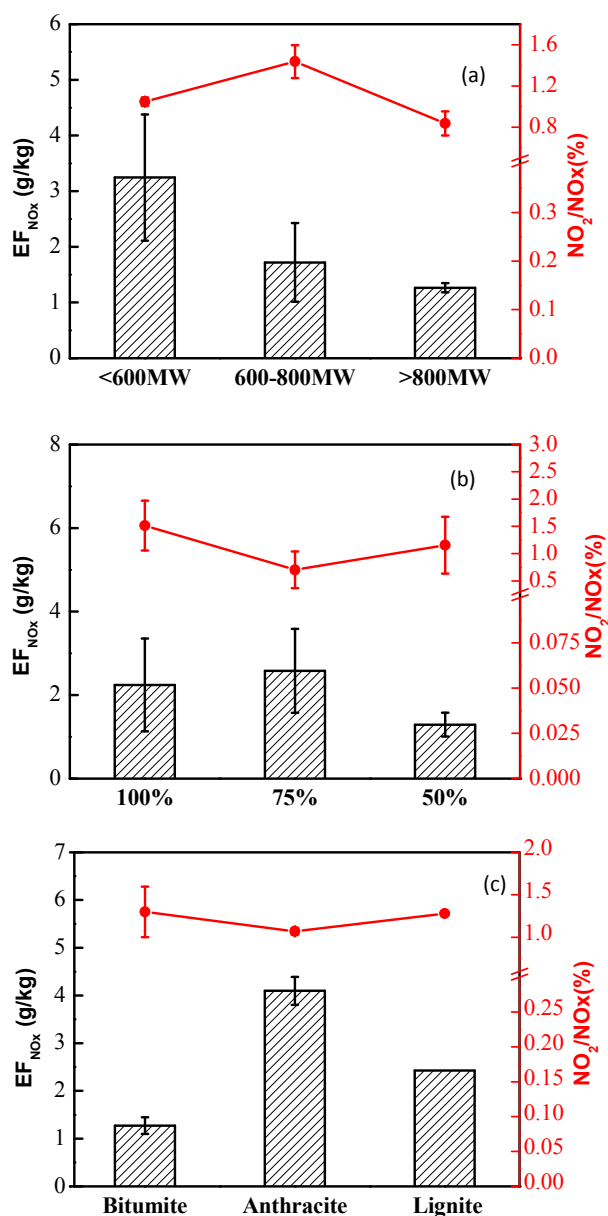


Fig. 3. NO<sub>x</sub> emission factors and NO<sub>2</sub>/NO<sub>x</sub> ratios under different conditions: (a) installed capacity; (b) operating load; and (c).

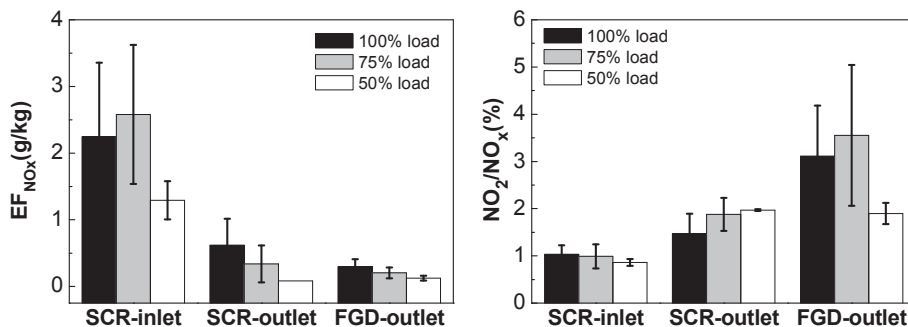


Fig. 4. NO<sub>x</sub> emission factors and NO<sub>2</sub>/NO<sub>x</sub> ratios at different sampling points.

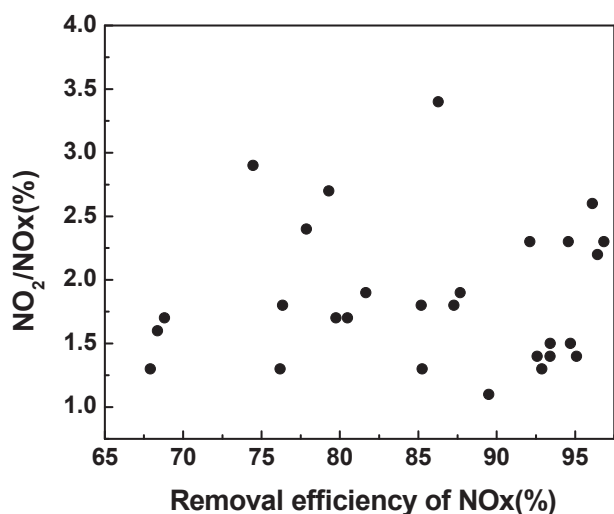


Fig. 5. Impact of SCR efficiency on NO<sub>2</sub>/NO<sub>x</sub> ratio.

the SCR outlet. Correspondingly, the NO<sub>2</sub>/NO<sub>x</sub> ratios increased (Fig. 4). In ESP system, some oxidants, especially ozone and free radical O, may generate (Awad and Castle, 1975; Liu et al., 2011; Yun et al., 2014), and partially oxidized NO to NO<sub>2</sub> during long residence time (around 20 s) (Lin et al., 2004; Wu et al., 2006). NO can also be partially oxidized to NO<sub>2</sub> in FGD system because of the presence of O<sub>2</sub> (Macneil et al., 1998; Zheng et al., 2014). However, both NO and NO<sub>2</sub> can be absorbed by limestone slurry following two pathways (Zheng et al., 2014), pure NO<sub>2</sub> absorption and simultaneous NO and NO<sub>2</sub> absorption. In this study, the newly generated NO<sub>2</sub> was greater than the consumed NO<sub>2</sub>, which leads to a small increase in the NO<sub>2</sub>/NO<sub>x</sub> ratio at the FGD outlet. However, the NO<sub>x</sub> emission factors were mostly constant and little affected by the FGD system. In addition, the influences of the ESP and FGD on the NO<sub>2</sub>/NO<sub>x</sub> ratios were small. All of the NO<sub>2</sub>/NO<sub>x</sub> ratios at the FGD outlet were less than 5%, which is in accordance with values reported in the AP-42 and used as a standard method in China.

Since the request to install APCDs in coal-power plants by the Chinese government, NO<sub>x</sub> emissions could have decreased. Considering the impacts of APCDs, the NO<sub>x</sub> emission factors at the FGD outlet in this study were 0.23–0.73 g/kg, depending on installed capacity, coal type, and operating load.

#### 4. Conclusions

Installed capacity, and coal type affected NO<sub>x</sub> formation. Larger units produced less NO<sub>x</sub>, and anthracite combustion generated

more NO<sub>x</sub> than bitumite and lignite combustion. However, these factors had little influence on the NO<sub>2</sub>/NO<sub>x</sub> ratios, which were all less than 2%.

The APCDs, especially SCR, decreased NO<sub>x</sub> emission factors but increased NO<sub>2</sub>/NO<sub>x</sub> ratios. However, NO<sub>2</sub>/NO<sub>x</sub> ratios were still less than 5%. The current method for calculating NO<sub>x</sub> emissions that ignores NO<sub>2</sub> is suitable for new coal-fired power plants.

This study also revealed that NO<sub>x</sub> emission factors produced by new power plants are lower than those of older facilities, which indicates that NO<sub>x</sub> emissions from current and future units will be overestimated if they are based on older emission factors.

#### Acknowledgements

The authors are grateful for the financial support of the National Basic Research Program of China (No. 2013CB228505). Any views and conclusions expressed in this article are those of the authors and do not necessarily reflect the views or policies of the Ministry of Science and Technology of the P. R. China.

#### References

- Adamowska-Teysier, M., Krztoń, A., Costa, P.D., Djéga-Mariadassou, G., 2015. SCR NO<sub>x</sub> mechanistic study with a mixture of hydrocarbons representative of the exhaust gas from coal combustion over Rh/Ce<sub>0.62</sub>Zr<sub>0.38</sub>O<sub>2</sub> catalyst. *Fuel* 150, 21–28.
- Awad, M.B., Castle, G.S.P., 1975. Ozone generation in an electrostatic precipitator with a heated corona wire. *J. Air Pollut. Control Assoc.* 25, 369–374.
- British Petroleum (BP), 2015. Statistical Review of World Energy 2015. <http://www.bp.com/en/global/corporate/about-bp/energy-economics/statistical-review-of-world-energy.html>.
- Busca, G., Lietti, L., Ramis, G., Berti, F., 1998. Chemical and mechanistic aspects of the selective catalytic reduction of NO<sub>x</sub> by ammonia over oxide catalysts: a review. *Appl. Catal. B-Environ.* 18, 1–36.
- Ciardelli, C., Nova, I., Tronconi, E., Chatterjeeb, D., Bandl-Konradb, B., 2004. A nitrate route for the low temperature fast SCR reaction over a V<sub>2</sub>O<sub>5</sub>–WO<sub>3</sub>–TiO<sub>2</sub> commercial catalyst. *Chem. Commun.* 23, 2718–2719.
- China State Electricity Regulatory Commission, 2011. Notification of Special Regulation for the Utilization Hour of Generation of Conventional Coal-fired Units with Capacity of More than 300 MW in China in 2010. The Situation of China. [http://www.china.com.cn/guoqing/zwx/2011-11/08/content\\_23859405.html](http://www.china.com.cn/guoqing/zwx/2011-11/08/content_23859405.html) (in Chinese).
- China State Council, 1999. Implementation Opinions of Accelerating Shutting Down Small Units. [http://www.gov.cn/zhengce/content/2008-03/28/content\\_2666.html](http://www.gov.cn/zhengce/content/2008-03/28/content_2666.html) (in Chinese).
- China State Council, 2007. Implementation Opinions of Accelerating Shutting Down Small Units. [http://www.gov.cn/zhengce/content/2008-03/28/content\\_2666.html](http://www.gov.cn/zhengce/content/2008-03/28/content_2666.html) (in Chinese).
- Fan, W., Lin, Z., Kuang, J., Li, Y., 2010. Impact of air staging along furnace height on NO<sub>x</sub> emissions from pulverized coal combustion. *Fuel Process. Technol.* 91, 625–634.
- Flagan, R.C., Seinfeld, J.H., 1988. *Fundamentals of Air Pollution Engineering*. New Jersey.
- Koebel, M., Elsener, M., Madia, G., 2001. Reaction pathways in the selective catalytic reduction process with NO and NO<sub>2</sub> at low temperatures. *Ind. Eng. Chem. Res.* 40, 52–59.
- Lei, P., 2012. Study on Emission Factor of NO<sub>x</sub> and Emissions of Thermal Power Industry. Doctorial Dissertation of Nanjing University of Information

- Technology, Nanjing. (in Chinese).
- Li, Z.Q., Liu, G.K., Zhu, Q.Y., Chen, Z.C., Ren, F., 2011. Combustion and NO<sub>x</sub> emission characteristics of a retrofitted down-fired 660 MWe utility boiler at different loads. *Appl. Energy* 88, 2400–2406.
- Lin, H., Gao, X., Luo, Z.Y., Cen, K.F., Huang, Z., 2004. Removal of NO<sub>x</sub> from flue gas with radical oxidation combined with chemical scrubber. *J. Environ. Sci.* 16, 462–465 (in Chinese).
- Liu, J.X., Han, Y.J., Mao, N., Chang, D.Q., Sun, X., 2011. Experimental Study on Ozone Generation in ESP. *China Environmental Protection Industry* (in Chinese).
- Macneil, J.H., Berseth, P.A., Westwood, G., Troglor, W.C., 1998. Aqueous catalytic disproportionation and oxidation of nitric oxide. *Environ. Sci. Technol.* 32 (7), 876–881.
- Olsson, L., Westerberg, B., Persson, H., Fridell, E., Skoglundh, M., Andersson, B., 1999. A kinetic study of oxygen adsorption/desorption and NO oxidation over Pt/Al<sub>2</sub>O<sub>3</sub> catalysts. *J. Phys. Chem. B* 103, 10433–10439.
- Sun, W.Y., Wang, Q.Y., Ding, S.L., Su, S.J., Jiang, W.J., Zhu, E.G., 2013. Reaction mechanism of NO<sub>x</sub> removal from flue gas with pyrolusite slurry. *Sep. Purif. Technol.* 118, 576–582.
- Sun, Y.Y., 2015. Study on Emission Inventory and Uncertainty Assessment of Multi-pollutants from Coal-fired Power Plants. Doctorial Dissertation of Zhejiang University, Zhejiang. (in Chinese).
- Tian, H.Z., Hao, J.M., Lu, Y.Q., Zhu, T.L., 2001. Inventories and distribution characteristics of NO<sub>x</sub> emissions in China. *China Environ. Sci.* 21, 493–497 (in Chinese).
- USEPA, 1998. External Combustion Sources, Emissions Factors & AP 42, Compilation of Air Pollutant Emission Factors, fifth ed. US Environmental Protection Agency.
- USEPA, 2014. Determination of Nitrogen Oxides Emissions from Stationary Sources (Instrumental Analyser Procedure). US Environmental Protection Agency.
- Wang, S.X., Zhang, L., Li, G.H., Wu, Y., Hao, J.M., Pirrone, N., Sprovieri, F., Ancora, M.P., 2010. Mercury emission and speciation of coal-fired power plants in China. *Atmos. Chem. Phys.* 10, 1183–1192.
- Wang, S.X., Yu, C., Hao, J.M., 2011. Control of NO<sub>x</sub> emissions from power plants: experiences of United States and its implications for China. *Chin. J. Environ. Eng.* 5, 1213–1220 (in Chinese).
- Wang, S.X., Hao, J.M., 2012. Air quality management in China: issues, challenges, and options. *J. Environ. Sci-China* 24, 2–13.
- Wang, J., Wang, Z.G., Zhao, B., Wang, S.X., Hao, J.M., 2014. Cost-effectiveness analysis of multi-pollutant emission reduction in power sector of China. *Res. Environ. Sci.* 27, 1314–1322 (in Chinese).
- Wang, Z.X., Zhao, Y., Pan, L., Liu, Z.Q., 2009. Study on the estimation methods for NO<sub>x</sub> emission from coal-fired power plants in China. *Electr. Power* 42, 59–62 (in Chinese).
- William, L., 1988. *Air Pollution Control Engineering*. New York and Basel.
- Wu, Z.L., Gao, X., Luo, Z.Y., Ni, M.J., Cen, K.F., 2006. Formation of ozone and NO<sub>x</sub> during corona discharge radical shower. *J. of Chem. Ind. Eng. (China)* 57, 1214–1219 (in Chinese).
- Xu, Y., Williams, R.H., Socolow, R.H., 2009. China's rapid deployment of SO<sub>2</sub> scrubbers. *Energy Environ. Sci.* 2, 459–465.
- You, Z., Wang, Z.H., Zhou, Z.J., Liu, J.Z., Zhou, J.H., Cen, K.F., 2011. NO emission during combustion of anthracite and bituminous coal in O<sub>2</sub>/CO<sub>2</sub> atmosphere. *Proc. CSEE* 31, 53–59.
- Yun, S., Park, J., Seo, Y., 2014. An experimental study for particle removal efficiency and ozone generation in electrostatic precipitation. *Int. J. Adv. Sci. Technol.* 2, 1–4.
- Zhang, Q., Streets, D.G., He, K.B., Wang, Y.X., Richter, A., Burrows, J.P., 2007. NO<sub>x</sub> emission trends for China, 1995–2004: the view from the ground and the view from space. *J. Geophys. Res. Atmos.* 112, 449–456.
- Zhao, Y., 2008. Study on Air Pollution Emission of Coal-fired Power Plants in China and its Environmental Impacts. Doctorial Dissertation of Tsinghua University, Beijing. (in Chinese).
- Zhao, Y., Wang, S.X., Nielsen, C.P., Li, X.H., Hao, J.M., 2010. Establishment of a database of emission factors for atmospheric pollutants from Chinese coal-fired power plants. *Atmos. Environ.* 44, 1515–1523.
- Zhao, B., Wang, S.X., Liu, H., Xu, J.Y., Fu, K., Klimont, Z., Hao, J.M., He, K.B., Cofala, J., Amann, M., 2013. NO<sub>x</sub> emissions in China: historical trends and future perspectives. *Atmos. Chem. Phys.* 13, 9869–9897.
- Zheng, C.H., Xu, C.R., Zhang, Y.X., Zhang, J., Gao, X., Luo, Z.Y., Cen, K.F., 2014. Nitrogen oxide absorption and nitrite/nitrate formation in limestone slurry for WFGD system. *Appl. Energy* 129, 187–194.
- Zhou, H., Yang, Y., Liu, H.Z., Hang, Q.J., 2014. Numerical simulation of the combustion characteristics of a low NO<sub>x</sub> swirl burner: Influence of the primary air pipe. *Fuel* 130, 168–176.